LEGIBILITY NOTICE

A major purpose of the Technical Information Center is to provide the broadest dissemination possible of information contained in DOE's Research and Development Reports to business, industry, the academic community, and federal, state and local governments.

Although a small portion of this report is not reproducible, it is being made available to expedite the availability of information on the research discussed herein.

LA-UR [illegible]

DEC 0 [illegible] 1989

Los Alamos National Laboratory is operated by the University of California for the United States Department of Energy under contract W-7405 ENG 36

LA-UR--89-4047

DE90 003221

TITLE ATOMIC PROCESSES IN PLASMAS UNDER ULTRA-INTENSE LASER IRRADIATION

AUTHOR(S) G. T. Schappert, D. E. Casperson, J. A. Cobble, J. C. Comly, L. A. Jones, G. A. Kyrala, K. J. LaGattuta, P. H. Y. Lee, G. L. Olson, A. J. Taylor

SUBMITTED TO AIP Conference Proceedings for 7th American Physical Society Topical Conference
Atomic Processes in Plasmas
Gaithersburg, Maryland

Submitted November 1989

MASTER

Los Alamos National Laboratory
Los Alamos, New Mexico 87545

ATOMIC PROCESSES IN PLASMAS UNDER ULTRA-INTENSE LASER IRRADIATION*

G. T. Schappert, D. E. Casperson, J. A. Cobble, J. C. Comly, L. A. Jones, G. A. Kyrala, K. J. LaGattuta, P. H. Y. Lee, G. L. Olson, and A. J. Taylor

Los Alamos National Laboratory
Los Alamos, New Mexico, 87545

ABSTRACT:

Lasers delivering subpicosecond pulses with energies of a fraction of a Joule have made it possible to generate irradiance levels approaching 10^{20} W/cm^2. We presently operate two such systems, a KrF based excimer laser capable of producing a few 10^{17} W/cm^2 at 248 nm with a repetition rate of 3-5 Hz and a XeCl based excimer laser capable of producing mid 10^{19} W/cm^2 at 308 nm and 1 Hz. We will discuss some experimental results and the theory and modeling of the interaction of such intense laser pulses with aluminum. Because of a small ASE prepulse the high intensity interaction is not at the solid surface but rather at the $n_e = 2\times10^{22}$ cm^{-3} critical density of the blowoff plasma generated by the ASE. The transient behavior of the plasma following the energy deposition by the intense subpicosecond pulse can be viewed as the energy-impulse response of the plasma. Experimental results and modeling of the x-ray emission from this plasma will be presented.

I. INTRODUCTION

Recent new developments in excimer laser technology have made it possible to achieve irradiances on target exceeding 10^{19} W/cm^2. The developments responsible for this are oscillator designs capable of generating pulses of the order of femtosecond duration and large aperture

amplifiers capable of amplifying these pulses without significant pulse stretching or optical distortion. Hence modest energies, e.g one joule in a 200 fs pulse, focused to a nearly diffraction-limited spot a few microns in diameter results in an irradiance of nearly 10^{20} W/cm^2. Such laser systems typically operate at a repetition rate of several Hz, ideal for experimental programs.

Laser matter interaction experiments and modeling of these experiments are in progress at several laboratories. Such experiments are of great interest because in this intensity range the radiation electric fields can exceed the atomic binding fields, leading to an area of atomic physics which has never been available for experimental study. At 10^{19} W/cm^2 the peak laser electric field is nearly 10^{11} V/cm, a factor of twenty larger than the basic atomic electric field unit e/a^2. The classical quiver energy of a free electron in such a laser field is 180 keV for the XeCl wavelength at 308 nm. Clearly, laser matter interactions under such conditions lead to ultrahigh energy density conditions in the material. In this paper we will describe the two high irradiance laser systems at Los Alamos and report on high energy density experiments in an aluminum plasma.

II. LASER FACILITY

Subpicosecond, high-brightness excimer laser systems are being used to explore the interaction of coherent ultraviolet radiation with matter. The vast majority of such systems, based on the amplification of subpicosecond pulses in small aperture (1 cm^2) XeCl or KrF amplifiers, deliver[1-4] focal spot irradiances of approximately 10^{17} W/cm^2. Scaling to higher irradiances requires an additional large aperture amplifier[5,6,7] which preserves nearly diffraction-limited beam quality and subpicosecond pulse duration. We describe both a small aperture KrF system which routinely provides irradiances $>10^{17}$ W/cm^2 to the experiments discussed here, as well as a large aperture XeCl system which produces 0.25-J, subpicosecond pulses and yields irradiances on target (with f/1 optics) of 6.4×10^{19} W/cm^2. The output parameters of both systems are summarized in Table I.

	LABS-I (KrF)	LABS-II (XeCl)
Repetition rate (Hz)	5	1
Wavelength (nm)	308	248
Energy (mJ)	30 ± 1	250 ± 10
Pulsewidth (ps)	.67	.335
Intensity (W/cm^2)	$4x10^{17}$ (f/3)	$6x10^{18}$ (f/3.7)
Intensity (W/cm^2)	$4x10^{18}$ (f/1)	$6x10^{19}$ (f/1)

Table I. Operating conditions of the Los Alamos Bright Source (LABS) laser systems LABS-I and LABS II.

The small aperture KrF system consists of a "front-end" which produces 248-nm seed pulses, followed by two KrF amplifiers. The system is sketched in Figure 1. The

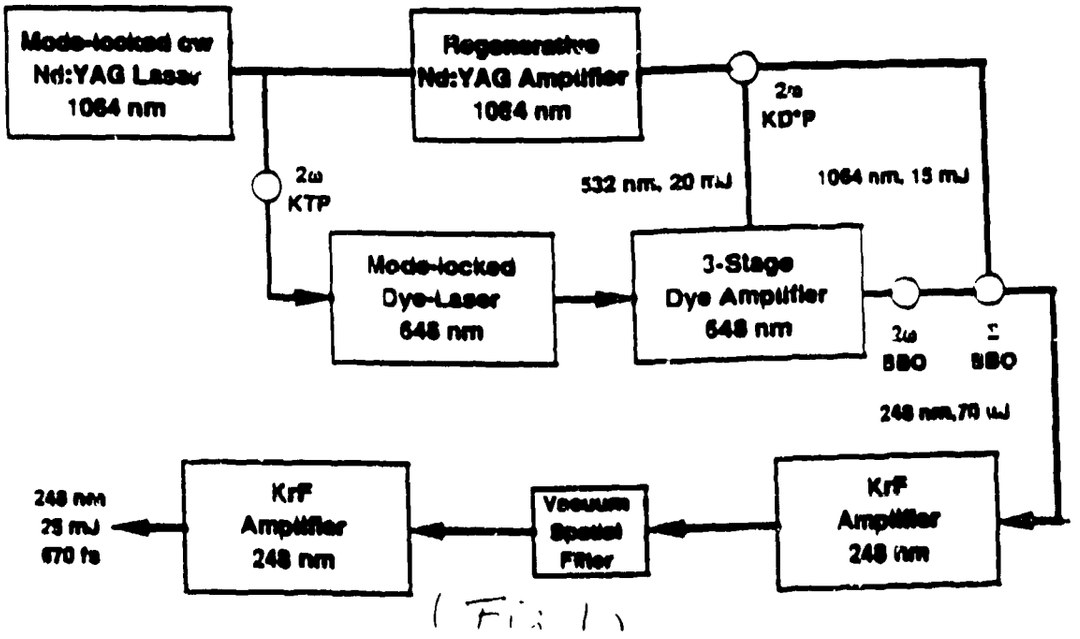

Fig 1. Small aperture high-brightness KrF laser system

output pulse train from a mode-locked Nd:YAG laser is split into two beams. One beam is frequency-doubled in KTP and used to synchronously pump a mode-locked dye laser with separate gain and absorber jets. The gain medium is DCM dissolved in benzyl alcohol and ethylene glycol, while the absorber is DTDCI in methanol and

ethylene glycol. A pulse from the remaining train is selected at a repetition rate of 5 Hz and amplified by a regenerative amplifier up to the 40-mJ level. This 100-ps pulse is frequency doubled in KD*P with 50% conversion efficiency and used to longitudinally pump a three stage dye amplifier seeded by the 650-fs, 648-nm pulses from the dye laser. The amplified pulse energy is 2.0 mJ and the beam quality is better than two times diffraction-limited. We observe no temporal broadening of the 650-fs pulses through the amplifier. Advantages of this synchronous amplification scheme include low spontaneous emission, nearly diffraction-limited amplified beam quality, elimination of timing jitter between the pump pulses and the seed pulses to the amplifier and the availability of the unconverted 100-ps, 1064-nm pulses for mixing purposes. The amplified 648-nm pulses are then frequency-doubled in a 2-mm long BBO crystal. The resulting pulses at 324 nm are finally sum-frequency mixed with unconverted 1064-nm pulses from the regenerative amplifier in a second 2-mm BBO crystal to produce 70-μJ subpicosecond seed pulses at 248 nm. This scheme, based on synchronous amplification, produces one to two orders of magnitude more energy in the 248-nm subpicosecond seed pulse than previously reported in other systems[2-6].

These pulses are then amplified by two Lambda Physik EMG 200 Series KrF amplifiers, separated by a vacuum spatial filter to suppress amplified spontaneous emission (ASE) and to improve beam quality. The output beam diameter is 25 mm and the final output energy is 30±1 mJ with <0.5 mJ ASE. The pulsewidth, measured using two-photon ionization in NO, is 670 fs. The focused spot size achievable with this system has been determined indirectly by measuring the confocal parameter of a beam focused by f/3 optics. The inferred focal spot diameter is 3.6 μm, which implies an irradiance at the focal plane of 4.4×10^{17} W/cm^2. For most experiments parabolic mirrors are used as the focusing optics to preserve pulsewidth, minimize aberrations and avoid nonlinear absorption and refraction.

The large aperture XeCl system[7] is sketched in Figure 2. Pulses of 165 fs duration at 616 nm are

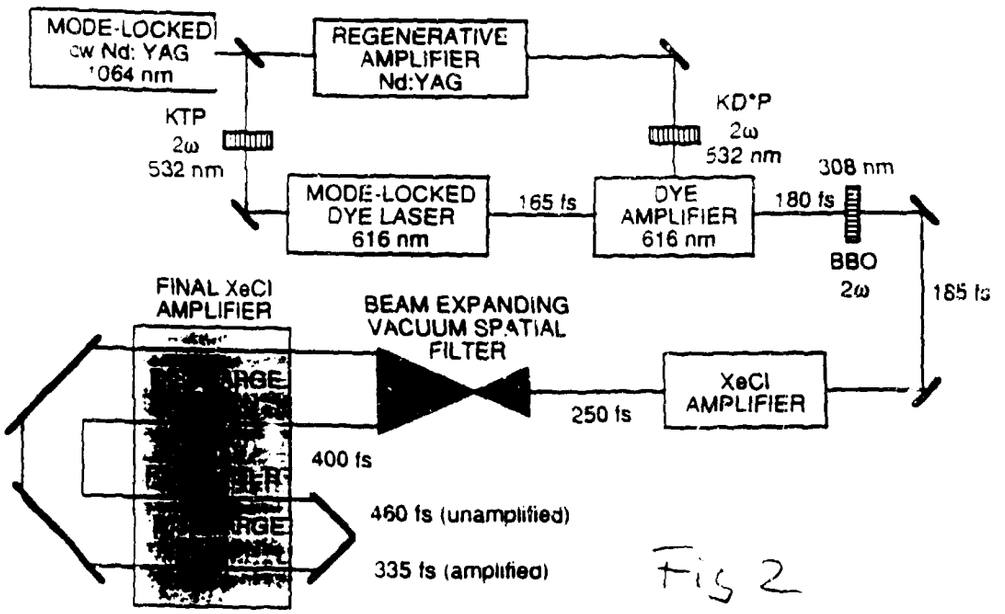

Fig. 2 Large aperture high-brightness XeCl laser system

initially generated in a linear-cavity, dispersion-compensated dye laser (Kiton Red/ DODCI) that is synchronously pumped by the frequency-doubled output of a cw mode-locked Nd:YAG laser. A synchronous amplification scheme, similar to that described for the KrF system, is used to amplify these pulses to the 1.5 mJ level[8]. The amplified 616-nm pulses are then frequency-doubled in a BBO crystal. Preamplification of these 0.15-mJ pulses to the 6-mJ level is accomplished with a single small aperture XeCl discharge laser. The pulsewidth at this stage is 250 fs. The beam is then expanded in a vacuum spatial filter before entering the final amplifier.

The 10x10 cm^2 aperture final amplifier consists of two independently pumped discharge gain regions, each sharing a common 130-keV x-ray preionizer. The discharges are pumped by low-jitter, thyratron-switched pulse modulators with two-stage magnetic compression. The resultant jitter is 5 ns over a 20-ns gain time. The small-signal gain length, g_oL, for each discharge region is 8.0 and useful gain is obtained over roughly one half of the aperture area. In order to maintain nearly diffraction-limited beam quality at a 1-Hz repetition rate, a gas flow system is employed which maintains

nearly laminar flow transverse to the discharge electrodes. After hot gas is cleared from the discharge volume, this flow system establishes less than $\lambda/20$ wavefront distortion over the clear aperture before the next shot is fired.

The output energy of the system is 250 ±10 mJ in a 335 fs pulse. To illustrate the evolution of the pulse shape as the pulse propagates through the system, the pulse duration at each stage has been indicated in Figure 2. All values given in the figure are measured using autocorrelation techniques (two photon ionization in DABCO), with the exception of the value given after the BBO doubling crystal, which was calculated. The ultrashort pulse lies on a 20-ns, 50-mJ ASE pedestal, but only half of the ASE is included in the solid angle of the output beam. The beam quality of the fully amplified pulse is determined by measuring the transmission through a calibrated pinhole using an f/3.7 focusing optic. The measured transmission of 82% through a 10 μm-diameter pinhole implies FWHM dimensions of the focal spot of 3.4±0.7 by 4.1±0.8 μm^2. These dimensions are about 3 times larger than would be obtained with a diffraction limited beam. With these focal spot dimensions, the mean focal irradiance is 4.6×10^{18} W/cm^2. To our knowledge, this represents the highest demonstrated optical irradiance ever obtained with a laser source. With f/1 focusing optics, this system will produce an irradiance of 6.4×10^{19} W/cm^2, which corresponds to an electric field of about 30 atomic field units and results in a relativistic electron quiver motion.

Initial experiments on this system have recently started. The first was a test of multiphoton absorption in Ne at an irradiance of several 10^{18} W/cm^2. The laser was focused into low pressure Ne (10^{-7}-10^{-6} Torr to avoid space-charge effects) in an ion time of flight spectrometer which separates the ions according to their charge to mass ratio. A typical time of flight spectrum is shown in Figure 3 indicating eight charge states of Ne and resolving the two isotopes ^{20}Ne and ^{22}Ne for most of them. To generate Ne^{+8} requires a net investment of more than 1 KeV of energy or the absorption of over 250 4-eV photons.

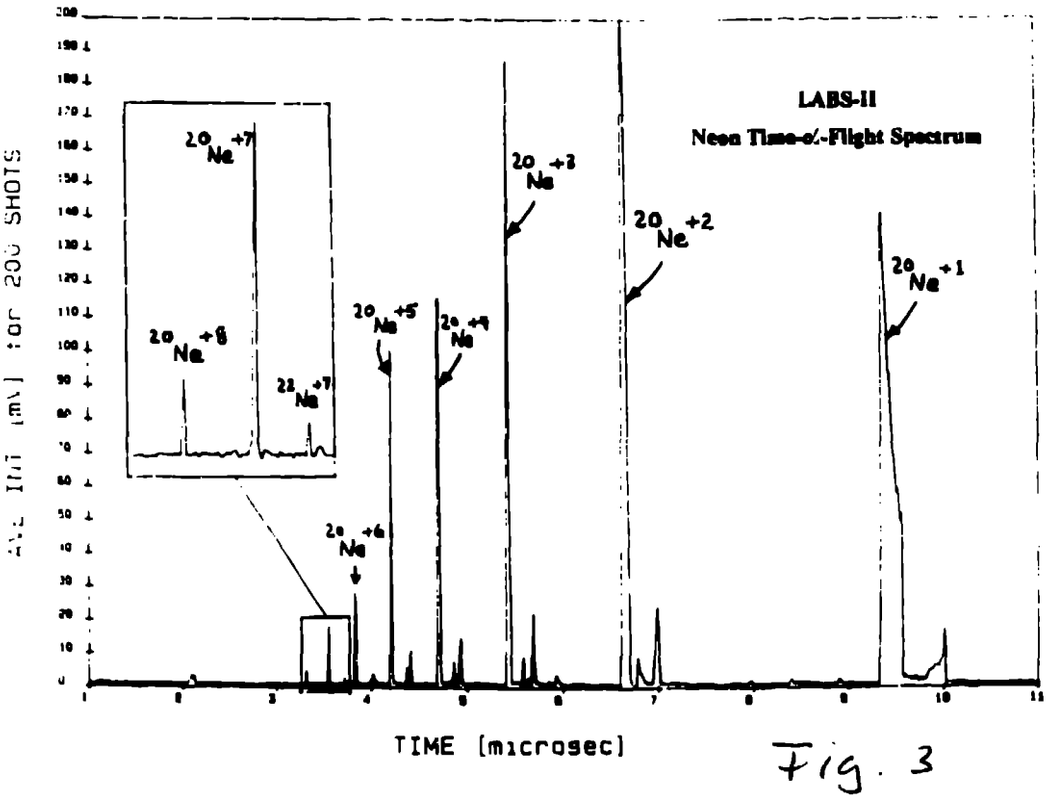

Fig. 3

II. SOLID TARGET EXPERIMENTS

The experiments discussed in this section are investigations of the interaction of high-irradiance pulses with solid targets performed on LABS-I. The purpose of this work is to study the resulting state of the hot, high-density plasma and possible applications.

A 20-mJ, 0.7-ps pulse is focused onto an aluminum target resulting in an irradiance of several 10^{17} W/cm^2 at a repetition rate of 3 Hz. The target slowly translates so that each pulse interacts with a new surface. The 0.7-ps main pulse is superimposed on a roughly 15-ns pedestal of amplified spontaneous emission (ASE) which contains about 5% of the total energy. Hence the main pulse interacts with a small blowoff plasma generated by this prepulse ASE. This raises the question whether the main pulse ever reaches the solid target surface since its propagation in the prepulse plasma is limited to electron densities below the 2×10^{22} cm^{-3} critical density. Since we cannot eliminate the ASE

prepulse, we have investigated its effect by varying the amount of ASE and the timing of the main pulse relative to the ASE onset. This gives rise to different scale-length prepulse plasmas in front of the solid.

The primary diagnostic on this experiment is x-ray spectroscopy. A transmission grating spectrograph is used to survey the plasma radiation from 5 to 100 Å with a resolution of 2 Å. We found substantial x-ray emission near 7 Å which corresponds to hydrogen- and helium-like aluminum emission. This spectral region around 7 Å is then investigated with a high-resolution flat PET crystal spectrograph covering 1.5 - 2 keV. The spectrum is shown in Figure 4 with the identification of several hydrogen-

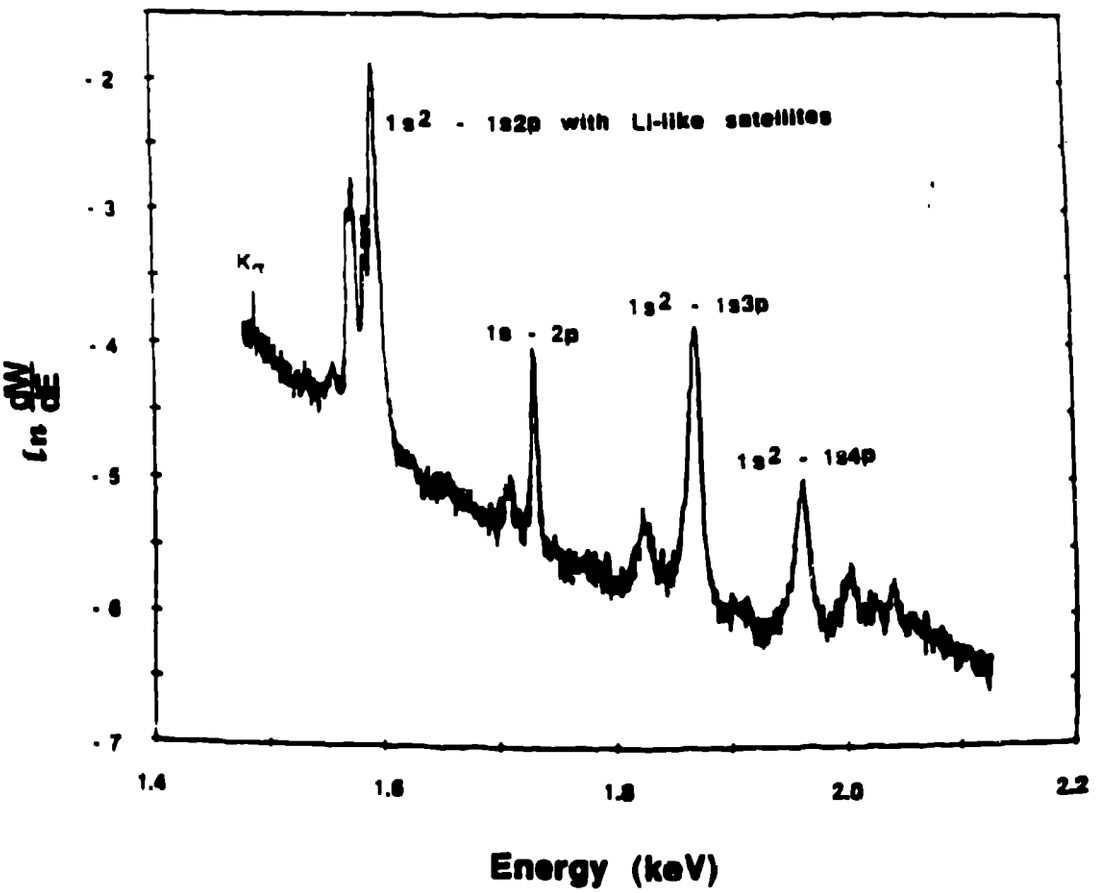

Fig.4 Natural log of x-ray flux from PET crystal spectrum of aluminum integrated over 100 shots

and helium-like aluminum lines. The spectrum is time integrated, requiring about one hundred shots. The temporal evolution of the 1.5-2 keV radiation is measured

with a filtered x-ray streak camera which indicated an emission time of less than 10 ps. Filtered pinhole camera pictures confine the emission region of this radiation to a spot of about 10μm in diameter.

A simple analysis[9] of this highly-transient non-equilibrium plasma based on the dominant collisional and radiative atomic rates resulted in a peak electron temperature of about 1.5 keV and an electron density near the critical density of 2 x $10^{22}/cm^3$. Preliminary estimates of x-ray conversion efficiency into keV line radiation approach 0.5 % of the laser energy.

We now turn to the investigation of the role of the ASE prepulse. By varying the ASE, we have subjected the aluminum surface to a prepulse intensity between 10 - 2000 GW/cm^2, resulting in various scale-length blow-off plasmas. Figure 5 depicts the typical situation, showing

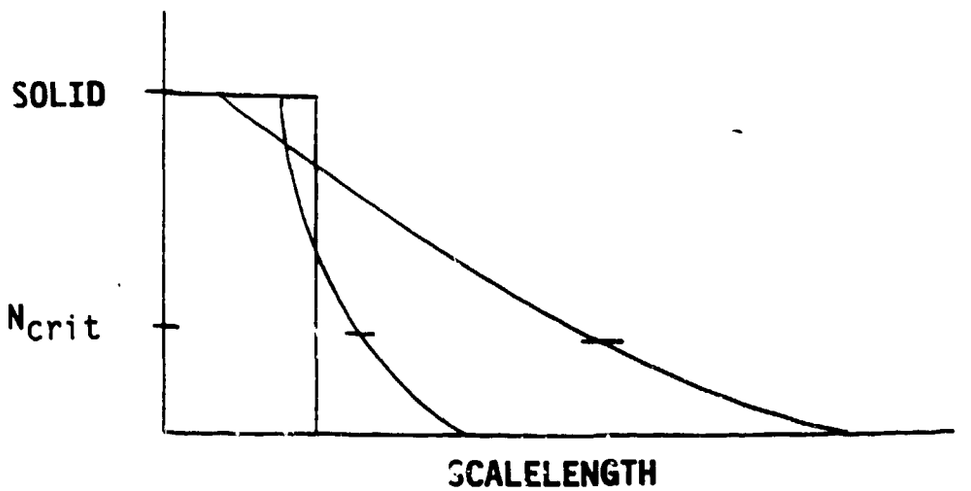

Fig.5 Blow-off plasma from ASE prepulse

the position of the initial solid aluminum boundary, a short scalelength blow-off plasma from a weak prepulse, and a long scale length plasma from a stronger prepulse. Since the lowest prepulse intensity (10 Gw/cm^2) is just about the damage threshold for aluminum, one would expect little if any blow-off and the interaction with the main pulse is close to solid density aluminum.

The PET crystal spectroscopy data were analyzed as function of the prepulse irradiance. We concentrate on the He-like Al 3-1 and 4-1 line intensities and the line widths. The instrumental width of the spectrometer is about 1 eV.

The intensities of the He-like Aluminum 3-1 and 4-1 lines are shown on Figures 6 a and b respectively. In

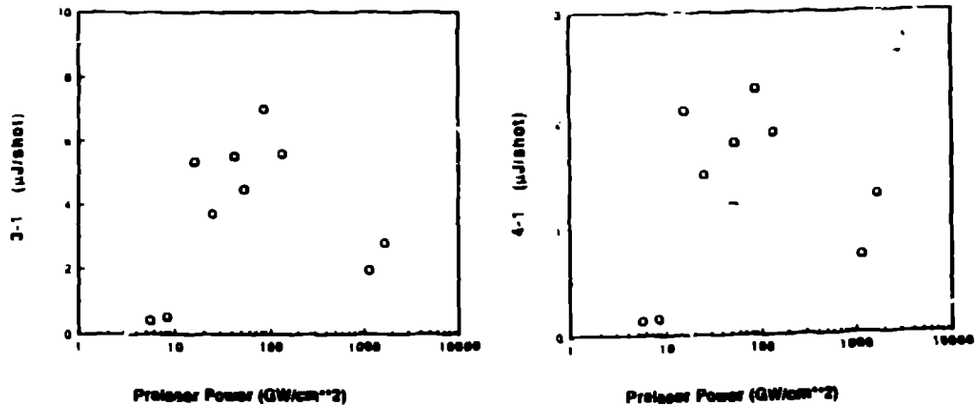

Fig.6 He-like Al (a) 3-1 line (b) 4-1 line intensity as a function of prepulse irradiance

both cases the intensities seem to require a threshold prepulse, peak at a moderate level of prepulse, and decline at high prepulse levels. A qualitative explanation of this dependence is that at low prepulse the energy is deposited in a steep density gradient at critical and transported by electron thermal conduction to the higher density region behind critical. The resulting lower electron temperature is insufficient to excite the He-like aluminum. At the other extreme, the main pulse is dissipated in the long density scale length plasma without reaching the critical density. Again, the lower temperatures cannot excite the emission. A similar effect has been observed [10,11] using short pulse dye lasers. The blow-off plasma was generated by a first pulse followed by a second pulse with adjustable delay. Neither paper studied individual spectral lines but broad band regions, the above 1 keV region in aluminum in ref(10) and the 35 - 70 eV region in tantalum in ref(11). From these results it is clear that there s an optimum prepulse plasma for maximum laser to x-ray conversion.

Figures 7 a and b show the linewidths (FWHM eV) of the 3-1 and 4-1 He-like lines respectively as a function of the prepulse irradiance. These lines have nearly the same linewidth, which appears to be inconsistent with Stark broadening theory with roughly n^2 scaling. An analysis of the widths based on scaling a He-like argon

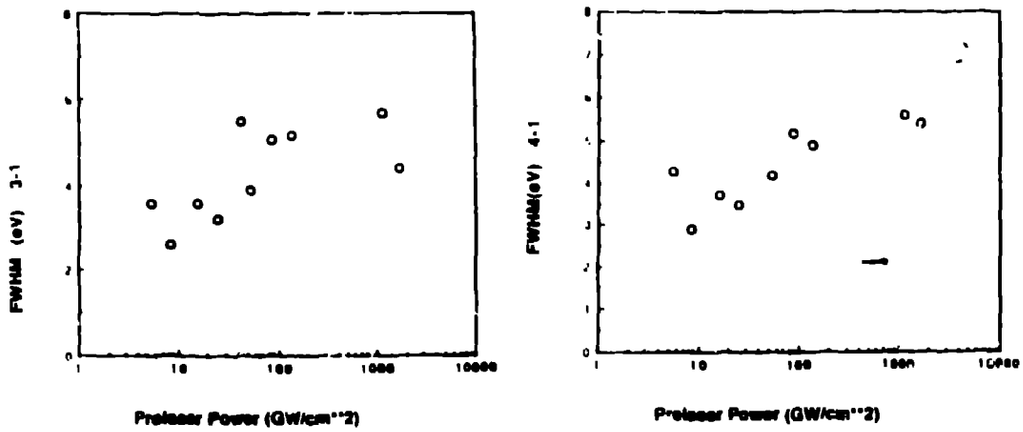

Fig. 7 He-like Al (a) 3-1 line (b) 4-1 line width FWHM(eV) as a function of prepulse irradiance

calculation[12] which includes electron broadening and ion dynamical effects is consistent with an electron density near n_{crit} (2×10^{22} cm^{-3}) for the 3 - 1 line, but about a factor of eight lower for the 4-1 line. This implies that the two lines are not emitted from the same region, or that substantial opacity broadening is involved in the 3-1 line emitted from the lower density region.

Next consider the factor of two increase in the linewidths as we increase the prepulse irradiance by over two orders of magnitude. Under the assumption of Stark broadening this implies an emission region of about three times the density at the highest prepulse irradiance compared to the lowest. At our lowest prepulse intensity we generate little or no plasma, hence the main pulse interacts at the critical density in the steep density gradient very near the solid aluminum. For a longer prepulse plasma scale length, the critical density region will be at a greater distance from the high density region resulting in less Stark broadening. A similar effect has been observed[13,14] in the soft x-ray emission from short pulse irradiated silicon. These experiments used a dye laser which was stated to have no prepulse. By introducing a prepulse, the plasma could then be investigated over a wide range of density gradients. Although the density diagnostic was not line width but resonance - intercombination line ratios, the

experimental results clearly indicated a narrower line width emission from what was interpreted as the higher density plasma, i. e. the no-prepulse case.

The above discussion questions whether the Stark effect is the dominant broadening mechanism for our He-like Al lines. The fact that the lines have nearly equal width suggests a motional effect. A simple Doppler interpretation would require ion temperatures of 15 - 60 KeV, which is unrealistic. Another possibility is the generation of large velocity fields. When the main pulse propagates up the prepulse generated plasma gradient a region of maximum energy deposition occurs. This is usually at critical if the pulse does not expend its energy earlier. The blow-off from this region then leads to a velocity field as shown in a one-dimensional ZAP-code simulation on Figure 8. A Gaussian prepulse of 10 ns

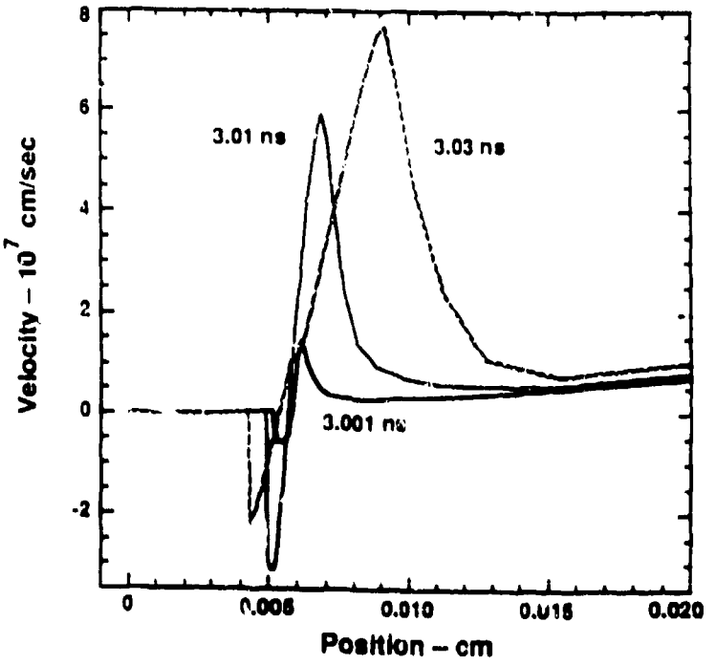

Fig.8 Calculated one dimensional velocity profile as a function of position 1, 10, and 30 ps after the main pulse

FWHM (truncated at itsFWHM) with peak intensity of 10^{11} W/cm^2 is incident on an Aluminum surface located at 0.005 cm. The ensuing absorption, hydro-blowoff, and heating are calculated. At 3 ns the .7 ps 10^{17} W/cm^2 main pulse

reaches the original solid interface after propagating through the blowoff plasma established by the prepulse. The plasma is further heated and ionized. Figure 8 shows the velocity fields at three different times after the main pulse. Note the large velocities established within a few ps of the main pulse near the solid interface and that the outgoing components are several times larger than those propagating into the high density material. The 1-2 keV radiation emitted from this region would be Doppler- broadened and blue-shifted by about 4 eV. Consider now the same problem with a long scale length prepulse plasma such that the critical density is far from the original solid interface. A more symmetric velocity field, with shocks running both up and down the gentle density gradient is established resulting in a Doppler spread (and no shift) of twice that of the steep gradient case. Hence, the results of this simulation show that hydro Doppler effects could explain the observed line width behavior provided they dominate the Stark broadening. This would require the emitting region be substantially below the critical density. Perhaps a Doppler-Stark coupling calculation[15] for He-like Al ions in a velocity field could resolve this problem.

More modeling and experimental work is in progress to resolve the above questions and lead to a better understanding of the role of prepulse plasmas in high irradiance laser matter interaction studies.

The role of multiphoton processes in the high density plasma interaction experiments is not clear. One might argue that if the collision frequency exceeds the optical frequency, the coherent interaction with the laser field is disrupted and multiphoton, or laser electric field dependent processes are diminished.

In general however, these results look promising for converting ps laser pulses into ps x-ray line radiation. We are presently investigating higher Z materials where one expects even better conversion efficiency. Such narrowband pulsed x-ray sources are valuable for applications such as x-ray laser research and time-resolved x-ray imaging.

IV. ACKNOWLEDGMENT

We wish to thank J. Grosso, S. E. Harper, T. R. Hurry, C. S. Lester, M. D. Maestas, J. P. Roberts, and K. A. Stetler for their technical support in laser operations and experiments and C. F. Fenstermacher and R. J. Jensen for their help in the design and procurement of the large amplifier for LABS-II.

* This work was supported by the U.S. Department of Energy under contract W-7405-ENG-36 with the University of California.

REFERENCES

1. J. H. Glownia, J. Misewich, and P. P. Sorokin, J. Opt. Soc. Am. B **4**, 1061 (1987).
2. A. P. Schwarzenbach, T. S. Luk, I. A. McIntyre, U. Johann, A. McPherson, K. Boyer, and C. K. Rhodes, Opt. Lett. **11**, 499 (1986).
3. J. R. Roberts, A. J. Taylor, P. H. Y. Lee, and R. B. Gibson, Opt. Lett. **13**, 734 (1988).
4. W. Tighe, C. H. Nam, J. Robinson, and S. Suckewer, Rev. Sci. Instrum. **59**, 2255 (1988).
5. J. R. M. Barr, N. J. Everall, C. J. Hooker, I. N. Ross, M. F. Shaw, and W. T. Toner, Optics Commun. **66**, 127 (1988).
6. A. Endoh, M. Watanabe, N. Sarukura, and S. Watanabe, Opt. Lett. **14**, 353 (1989).
7. A. J. Taylor, J. P. Roberts, T. R. Gosnell, and C. S. Lester, Opt. Lett. **14**, 444 (1989).
8. A. J. Taylor, C. R. Tallman, J. P. Roberts, C.S. Lester,T. R. Gosnell, P. H. Y. Lee, and G. A. Kyrala to be published in Optics Letters, January 1990
9. J. A. Cobble, G. A. Kyrala,A. A. Hauer,A. J. Taylor, C. C. Gomez, N. D. Delamater, and G. T. Schappert Phys. Rev. A. **39**, 454, (1989)
10. D. Kuhlka, U. Herpers, and D. von der Linde Appl. Phys. Lett. **50**, 1785, 1987
11 H. W. K. Tom and O. R. Wood,II Appl. Phys. Lett. **54**, 517, 1989
12. H. R. Griem, M. Blaha, and P. C. Kepple

Plasma Preprint UMLPR 89-029
13. M. M. Murnane, H. C. Kapteyn, and R. W. Falcone
Phys. Rev. Lett. **62**,155, 1989
14. H. M. Milchberg and H. R. Griem
Phys. Rev. Lett. **63** ,338,(1989)
15. R. Stamm, B. Talin, E. L. Pollock and C. A. Iglesias
Phys. Rev. A. **34**, 4144, 1986